Applied Surface Science 443 (2018) 374–381

Contents lists available at ScienceDirect

Applied Surface Science

journal homepage: www.elsevier.com/locate/apsusc

Full Length Article

Synthesis of cellulose diacetate based copolymer electrospun nanofibers for tissues scaffold

Wencheng Liang [a], Jia Hou [a], Xiangchen Fang [b], Fudong Bai [b], Tonghe Zhu [c], Feifei Gao [a], Chao Wei [a], Xiumei Mo [c], Meidong Lang [a,*]

[a] Shanghai Key Laboratory of Advanced Polymeric Materials, Key Laboratory for Ultrafine Materials of Ministry of Education, School of Materials Science and Engineering, East China University of Science and Technology, 130 Meilong Road, Shanghai 200237, PR China
[b] Fushun Research Institute of Petroleum and Petrochemicals, SINOPEC, 31 Dandong Road, Fushun 113001, Liaoning, PR China
[c] State Key Laboratory for Modification of Chemical Fibers and Polymer Materials, College of Chemistry, Chemical Engineering and Biotechnology, Donghua University, Shanghai 201620, PR China

ARTICLE INFO

Article history:
Received 7 January 2018
Revised 7 February 2018
Accepted 8 February 2018
Available online 10 February 2018

Keywords:
CDA-*g*-PET
Graft copolymer
Electrospinning
Hemolysis
Biocompatibility

ABSTRACT

In this study, a novel cellulose diacetate based copolymer used as tissues scaffold, cellulose diacetate-graft-poly(ethylene terephthalate) (CDA-*g*-PET) was developed by "graft onto" strategy using 3-Isocyan atomethyl-3,5,5-trimethylcyc-lohexyl isocyanate (IPDI) as a coupling reagent of cellulose diacetate and poly(ethylene terephthalate), and using dibutyltin dilaurate (DBTDL) and 1-butyl-3-methylimidazolium chloride salt ([Bmim]Cl) as catalysts. CDA-*g*-PET copolymers with five different grafting ratios were obtained by the regulation of the reaction time. It was proved by the FT-IR spectra of the purified copolymers that PET had been successfully grafted onto CDA backbone. Afterwards, CDA-*g*-PET nanofibers were fabricated via electrospinning and further were cross-linked by means of treating in glutaraldehyde (25%wt) aqueous solution for 48 h. The uniform and smooth fiber morphology was proved by SEM and the diameter decreased with the increase of grafting ratio. Moreover, the value of TGA revealed that the grafting PET onto CDA backbone would improve heat-resistant quality of CDA and help to improve the ability of thermo processing. The graft of PET onto CDA significantly enhanced mechanical property of copolymer compared with CDA. The results of hemolysis ratio indicated that hemolysis ratio has decreased compared with CDA, highlighting the potential application in the field of contacting with blood. In vitro cell viability indicated that CDA-*g*-PET would enhance biocompatibility compared with CDA.

1. Introduction

In recent years, cellulose has drawn more and more attention due to its abundant source, high biocompatibility, biodegradable and other excellence properties. Among them, cellulose diacetate (CDA), with the average degree of substitution (DS) ranging from 2.2 to 2.7 acetyl groups per glucose group, has been widely used in the scope of cigarette tows [1], biosensor [2] and membrane separation. Processing methods of CDA were mainly divided into thermo process and solution method. Because a great quantity of polar groups located on CDA, such as ethanoyl and hydroxyl generally cause strong intra- and intermolecular forces, leading to very high flow temperature (T_f) close to thermo degradable temperature (T_m), conventional thermal process is inappropriate [3]. Therefore, solution method such as electrospinning [4], drying spinning [5] and wetting spinning [6] would be more popular, especially in tissues scaffold. However, original CDA has low mechanical property [7], which limits its widely application in tissues scaffold. To improve mechanical property for tissues scaffold, CDA fibers prepared by solution method are blended with high mechanical property polymers in commercial spinning, such as polycarbonate (PC), nanocrystals (CNC) and others petroleum-based polymers. For example, Soyama et al., used polyester resins (PAA, PBSA) and glass fibers to improve the mechanical property of cellulose diacetate, and the results showed that the blending strength and impact strength were markedly improved [8].Ye et al., reported the simply blending of CDA/epoxy resin (EP) and curing with isophorone diamine (IPDA), and the results showed that the tensile strength, flexile strength, flexile modules and hardness of CDA/EP cross-linked by IPDA were higher than pristine CDA and the simple CDA/EP binary blend [5]. However, the composite materials by

* Corresponding author.
E-mail address: mdlang@ecust.edu.cn (M. Lang).

https://doi.org/10.1016/j.apsusc.2018.02.087
0169-4332/

blending usually show poor interface compatibility and short-life in application. Therefore, chemical modification of CDA with functional polymer or polymer resins are widely used in commercial production and research [9]. Such as, Guillaume et al., demonstrated the successfully grafting polystyrene onto cellulose acetate (CA-*g*-PS), and the enhanced mechanical properties after grafting [10]. Yuan et al., synthesize the CDA-SiO_2 composite coating material to improve the electrolyte wettability and the thermal stability of Li^+-ion battery separators [11].

Polyethylene terephthalate (PET) has been widely used as reinforcing material because of its good mechanical property. PET was measure as 115 MPa of tensile strength and attracted much attention as a reinforce material [12]. However, poor biological property has limited widely application in the scope of tissues scaffold [13]. So developing novel methods to improve its biological property is a fundamental requirement. For example, Nina Recek et al., successfully modified PET surface by SO_2/O_2 mixture gas plasma to promote cell proliferation [14]. Pezzoli et al., changed inertness of PET and promoted PET biological property through gelatin coating on PET fiber surface [15]. It should be noted that, to date however, there are no reports describing the modification of PET using CDA.

Electrospinning (ES) is an effective and facile way to fabricate a large quantity of nanofibers for the application in commerce and investigation such as filtration [16,17], drug delivery [18], chemical catalyze [19], biology [20,21] and so on, due to its easy operate and control. Generally, ultrathin fibers prepared by ES with the diameter ranging from nanometer to sub-micrometer show excellent properties, such as large surface area per unit volume, high degrees of interconnection and porous structure, which can mimics the structure of native ECM [22]. Different microstructure of fibers can be processed by tuning the configuration of spinning apparatus, such as core-shell fiber, hollow fiber and three-dimensional fiber scaffold. The morphology of nanofibers may be affected by many experimental parameters, such as polymers (types, molecular weight), solvents (types, diffusion in air, polarity), solution properties (concentration, viscosity, electric conductivity), process parameters (voltage, feed rate of solution, needle-collector distance, ambient condition) [23–27].

Tissue engineering scaffold is a kind of biomimetic technology, which designed material enable active control of cell behaviors and tissue/organ function, and thereby synergistically facilitate host-initiated repair/healing/regeneration [28]. Therefore, in this study, a novel cellulose diacetate based copolymer with excellent biocompatibility of CDA and the excellent mechanical properties of PET was synthesized by graft-onto reaction. The nanofibers of CDA-*g*-PET were fabricated via electrospinning. The structure and thermal properties of CDA-*g*-PET were investigated. Then nanofiber membranes were investigated by scanning electron microscopy (SEM) and water vapor transmission rate (WVTR) and so on. The results of hemolysis ratio (HR) and cell viability, showed that grafting PET onto CDA backbone could decrease hemolysis and enhance biocompatibility than CDA, they are very important for tissues scaffold.

2. Materials and methods

2.1. Material

Polyethylene terephthalate (PET, Mn = 4000 g/mol) was self-synthesized in lab. Cellulose diacetate (CDA, DS = 2.7, Mn = 100,000 g/mol) was purchased in Beijing Enoch technology co. Ltd. 1,1,2,2-tetrachloroethane ($C_2H_2Cl_4$, AR, 98%), isophorone diisocyanate (IPDI, AR, 98%) and dibutyltin dilaurate (DBTDL, AR, 98%) were purchased in Shanghai Ling Feng reagent co. LTD, six fluorine isopropyl alcohol (HFIP, AR, 98%) and 1-butyl-3-methyl-imidazole chloride ion liquid ([Bmim]Cl, AR, 98%) were purchased in Shanghai Teng Hui Biotechnology co. Ltd. Methylene dichloride (CH_2Cl_2, AR, 98%), petroleum ether (MSO, AR, 98%) were purchased in Guo Yao group reagent co. Ltd.

2.2. Preparation of CDA-g-PET

CDA powders was dissolved in $C_2H_2Cl_4$ and stirred for 2 h under nitrogen to obtain a homogenous solvent. PET was added into $C_2H_2Cl_4$ in a single-mouth flask and mixed by stirring to obtain a fully dissolved solution under nitrogen at 70 °C, then coupling reagent IPDI, catalyst DBTDL and [Bmim]Cl were added to PET solvent to modify the end group (OH) for 6 h, which can make the reaction of OH and NCO. Then the CDA dissolved in $C_2H_2Cl_4$ was added to the PET solvent and react for 1 h, 2 h, 5 h, 10 h and 24 h, CH_2Cl_2 and MSO were added to the mixture under stirring to precipitate out the production of CDA-*g*-PET. Finally, the precipitate was filtered, washed repeated with CH_2Cl_2 and MSO solvent and dried in vacuum oven at room temperature for 48 h until constant weight, which were called CA^a, CA^b, CA^c, CA^d and CA^e, respectively.

2.3. Electrospinning

Polymer was dissolved in HFIP at a steady stirring speed to reach a homogeneous solution, then the mixed solution was placed at room temperature to remove its air bubbles. The ES nanofibers were processed at room temperature with a needle-collect distance of 15 cm, polymer solution (CDA and CDA-*g*-PET) were transferred into a 5 ml plastic syringe equipped with a stainless steel flat-tip needle (0.21 mm inner diameter), and polymer fibers were collected on the collector plate of tin foil paper at a feed ratio of 0.5 ml/h controlled by a syringe pump during the time span of 10 h. The electric field was provided by a 16 kV high voltage power. HFIP evaporates during the flight of the fibers from the syringe to the collector plate. The as-spun fibers were put into vacuum oven for 48 h at room temperature to remove residual HFIP. The sample crosslinks with 25%wt glutaraldehyde aqueous solution in sealed dryer. Once removed from the dryer, the membranes were washed by ethanol to remove cross-linking agent and put into oven for 1 h at room temperature again.

2.4. Fourier transform infrared spectroscopy (FT-IR)

The FTIR spectra of pristine CDA, pristine PET and CDA-*g*-PET were carried out on FTIR Spectrometer (Nicolet 6700, American) with an accuracy of 4 cm^{-1}, measured on scanning range from 700 cm^{-1} to 4000 cm^{-1}, the solid samples were grinded well with KBr press to prepare pellets.

2.5. The measurement of grafting ratio (GR)

Pure the graft copolymer CDA-*g*-PET from drying in vacuum oven till constant weight, afterwards, weigh the polymer, calculate grafting ratio by the following Eq. (2.5).

$$GR = \frac{W_3}{W_1 + W_2} \times 100\% \tag{2.5}$$

where w_1, w_2, w_3 were the weights of CDA, PET and CDA-*g*-PET, respectively.

2.6. Thermogravimetric analysis (TGA)

The TGA of pristine CDA, pristine PET and CDA-*g*-PET were performed using a TA Q500 instruments. The samples were heated

from 50 °C to 600 °C at the heating rate of 10 °C·min^{-1} in dynamic nitrogen atmosphere.

2.7. Scanning electron microscope (SEM)

The fibrous morphology of pristine CDA and CDA-*g*-PET were observed by SEM (JCM-6000, Japan) at an accelerating voltage of 10 kV, all samples were gold sputter coated 30 s under argon in order to produce electric conductivity. The diameter was measured by SEM on different parts of 100 fibers. And then use Image J (National Institute of Health, USA) software to get statistical fiber diameters and resort to origin 8.0 to calculate fiber diameter distribution.

2.8. Mechanical property

The tensile strength and elongation of pristine CDA and CDA-*g*-PET were performed by universal tensile tester (2K WCMT 2203, China) at a tensile speed of 10 mm·min^{-1}, all samples for mechanical test are shaped in rectangular shape ($25 \times 4 \times 0.05$ mm^3), the result was the average value of at least three test values.

2.9. Water contact angle

The wettability of the prepared pristine CDA and CDA-*g*-PET membranes were measured at room temperature and 50% humidity by automatic contact angle meter (JC2000D2, China) which deionized (DI) water drop size was 0.1 ml, the result of contact angle was the average value of at least three test values at different locations on the per membrane.

2.10. Water vapor transmission rate (WVTP)

WVTR is determined by the American standard method E96-00 at 37 °C and 85% humidity for 24 h. Briefly, membrane samples (thickness of 0.1 mm ± 0.015 mm) of CDA and CDA-*g*-PET were sealed over the circular opening of glass tubes (diameter of 13 mm) filled with 10 ml DI water, those tubes were kept in sealed constant temperature humidity chamber which contains a saturated solution of ammonium sulfate and maintains the temperature of 37 °C and the humidity of 85% [29]. The WVTR (g·m^{-2}·day^{-1}) was calculated by the following equation:

$$WVTR = \frac{W_0 - W_f}{AT}$$

where A was the tube mouth (m^2), T was the trial time, W_0 and W_f were the weights of trial before and after, respectively.

2.11. Hemolysis rate analysis

Each of fiber mat samples (circle-shape of 9 mm diameter) was dipped in normal salt solution bath and incubated at 37 °C for 24 h previously. And then nanofiber mats incubate in 0.2 ml fresh anti-coagulated blood and 10 ml normal salt solution. Additionally, prepare 10 ml normal salt solution with 0.2 ml fresh anti-coagulated blood and DI water with 0.2 ml fresh anti-coagulated blood as negative control group and positive control group, respectively. Finally, all samples incubate at 37 °C for 1 h. After the incubation, remove the membranes, all tubes of sample centrifuge at 2000 rpm for 10 min, and the absorbance was measured by UV–Vis (SP-1900, China) at 545 nm, the hemolysis rate was calculated through the following equation:

$$HR = \frac{D_t - D_e}{D_p - D_e} \times 100\%$$

where D_t, D_e, D_p were the absorbance of test sample, negative control group and positive control group, respectively.

2.12. Biocompatibility

The biocompatibility of pristine CDA and CDA-*g*-PET were measured by the adhesion and growth of L929. Fibroblast were seeded in the 24-well plates at a concentration of 20,000 cells/well, circle-shape membranes of CDA and CDA-*g*-PET with 14 mm diameter were sterilized by UV radiation for 48 h, and then placed in the wells with attaching cells. In addition, cells were seeded in a blank well as blank control. All cells grew at 37 °C incubator in a humidified atmosphere of 5% CO_2 for 1, 3 and 7 day. The viability of cells was evaluated by MTT, the optical density (OD) values were measured at 490 nm, the percent viability was calculated by following equation:

$$cell\ viability = \frac{OD_t}{OD_c} \times 100\%$$

where OD_t was the absorbance of CDA or CDA-*g*-PET at 490 nm, OD_c was the absorbance of blank control group at 490 nm.

2.13. Statistical analysis

Origin 8.0 (origin Lab Inc, USA) was applied for helping statistical analysis, all the results were expressed as means ± standard deviation (SD), statistical differences determined by the one way analysis of variance (ANOVA) were considered significant at $p < 0.05$.

3. Result and discussion

3.1. The preparation and characterization of CDA-g-PET

Used as tissues scaffold, excellent mechanical properties and biocompability are very important. In this study, to improve the mechanical property and biocompability of CDA, we try to fabricated novel CDA-based polymer CDA-*g*-PET by grafting PET onto CDA backbone using IPDI as coupling reagent, DBTDL and [Bmim]Cl as catalysts, schematic illustration as show in Fig. 1a. Fig. 1b shows the optical image of CDA-*g*-PET copolymer nanofiber membrane, which indicated that the cellulose diacetated based copolymer nanofiber membrane could be prepared in large scale via electrospinning.

Chemical structure of copolymers was characterized by FTIR spectroscopy, as shown in Fig. 2. Fig. 2a showed the FTIR spectrum of CDA. The absorbance peaks of acetyl group (CHCOO) were observed at 1753 cm^{-1}, 1370 cm^{-1} and 1239 cm^{-1} corresponding to C═O, C—O, C—H. and 3487 cm^{-1} and 1048 cm^{-1} were represented to the hydroxyl and ring of cellulose ether, respectively. Fig. 2b showed the FTIR spectrum of PET, where 3430 cm^{-1} was assigned to the O—H in the end of PET, 1722 cm^{-1} and 1042 cm^{-1} were attributed to C═O and C—O, 2963 cm^{-1} and 2903 cm^{-1} were attributed to the CH_2 asymmetric stretching and CH_2 symmetric stretching [30]. Compare with CDA and PET, a new peak at 1548 cm^{-1} was corresponded to the amide NH group and 3425 cm^{-1}, 2918 cm^{-1}, 1716 cm^{-1}, 1206 cm^{-1}, 1064 cm^{-1}, 966 cm^{-1} were corresponded to NH, CH_2, C═O, C—O, ring of cellulose ether and Ar—H, respectively (Fig. 2C), which suggested the successful preparation of CDA-*g*-PET.

To get grafting ratio change with time, we calculated the mass change of CDA, PET and CDA-*g*-PET, and then obtained grafting ratio according to Eq. (2.5). As shown in Fig. 3, the grafting ratio increased with reaction time, but became almost constant after 10 h, which is owing to the steric hindrance increased with the

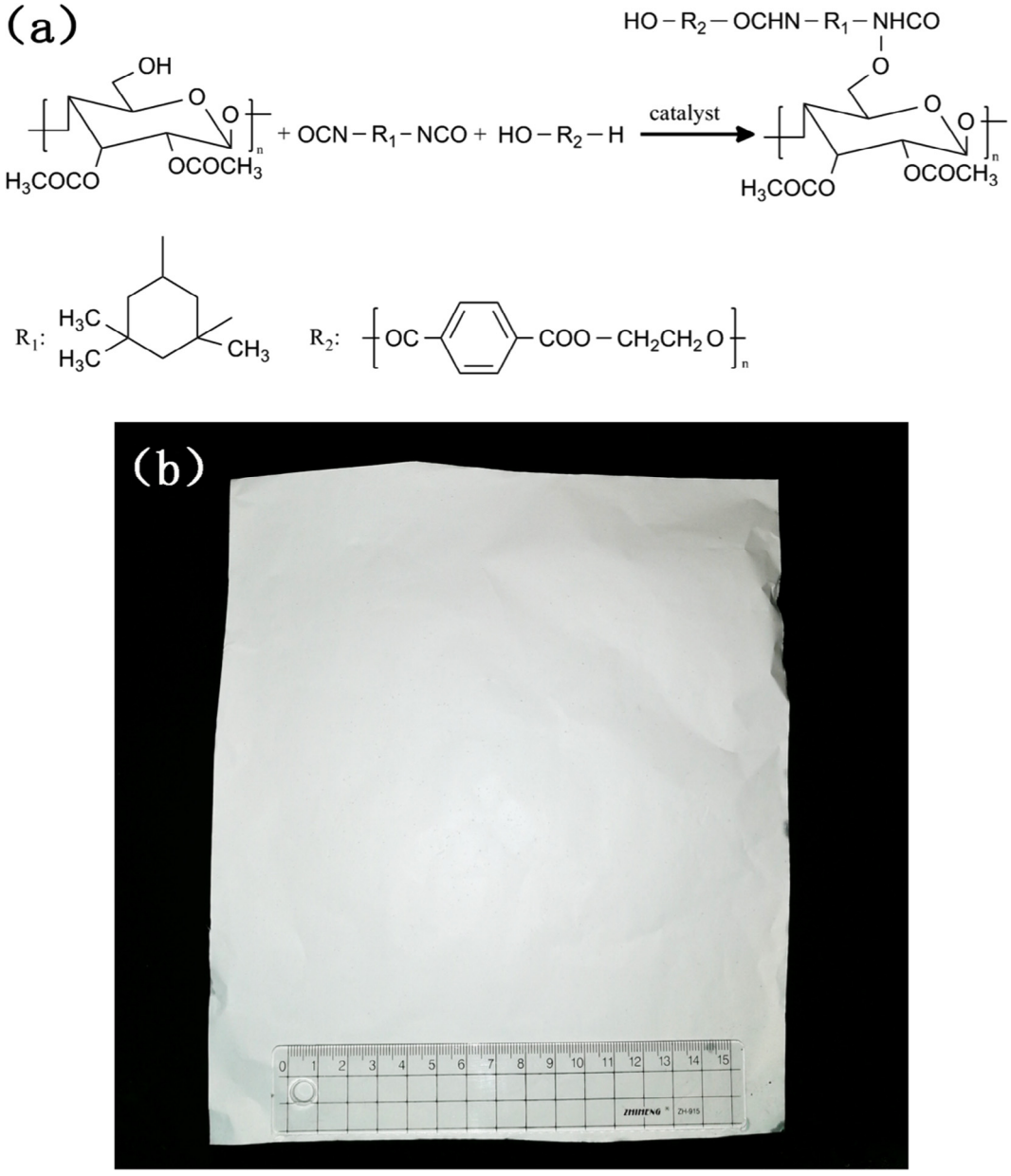

Fig. 1. (a) Schematic illustration for synthesis of CDA-*g*-PET, (b) optical image of CDA-*g*-PET copolymer nanofiber membrane.

grafting time. Briefly, PET is a long linear molecular chain and beneficial to the grafting reaction at low grafting ratio and low steric hindrance, as grafting reaction time goes by, especially over 10 h, high steric hindrance will impede grafting reaction. Especially, the samples at 1 h, 2 h, 5 h, 10 h and 24 h of grafting time were named as CA^a, CA^b, CA^c, CA^d and CA^e, respectively.

The thermo stability is an important factor as it influences process and use. The molecular chains of CDA contain a large number of polar groups such as ethanoyl groups and hydroxyls that can reduce the thermo stability and accelerate the aging of CDA when subjected to high temperature. To determined the thermo stability of CDA-g-PET. The thermal stability of CDA, PET and CDA-g-PET were measured by thermogravimetric analysis (TGA). As shown in Table 1. The decomposition onset temperature of CDA is 268 °C, while PET is 380 °C which are consistent with the previous reports [21,30]. Importantly, the thermo stability of CDA-g-PET was significantly improve and the decomposition onset temperature increased with grafting ratio, while the cellulose diacetate based copolymer maximum decomposition temperature and final decomposition temperature were closed with pristine cellulose diacetate. Indicating that grafting PET onto CDA backbone will improve the heat-resistance quality of CDA, which are significative in improve the ability of thermo processing and using [31].

3.2. Fabrication and characterization of nanofiber membrane

Fabricate nanofiber membrane was fabricated via electrospinning using HFIP as solvent, then crosslinking with glutaraldehyde aqueous solution for 48 h. SEM was used to observe the morphology of membrane and statistical nanofiber diameter distribution. Results as shown in Fig. 4, it can be observed that the fibers are uniform, bead-free and random oriented. The average diameters of CDA, CA^a, CA^b, CA^c, CA^d and CA^e were 1.61 μm, 1.40 μm, 1.14 μm, 1.02 μm, 1.09 μm and 0.80 μm, respectively. The result

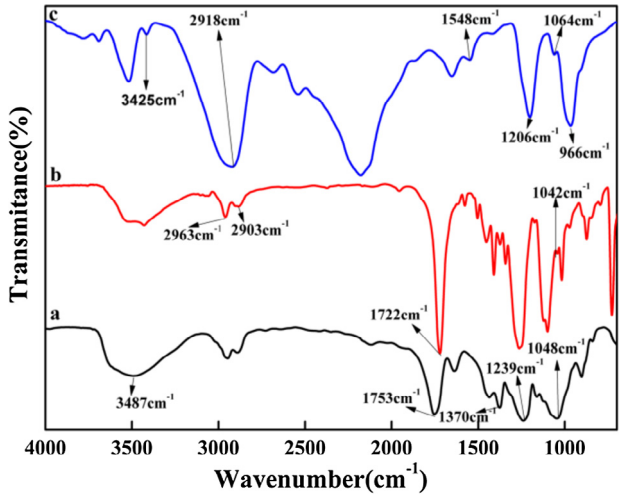

Fig. 2. FTIR spectra of (a) CDA, (b) PET and (c) CDA-*g*-PET.

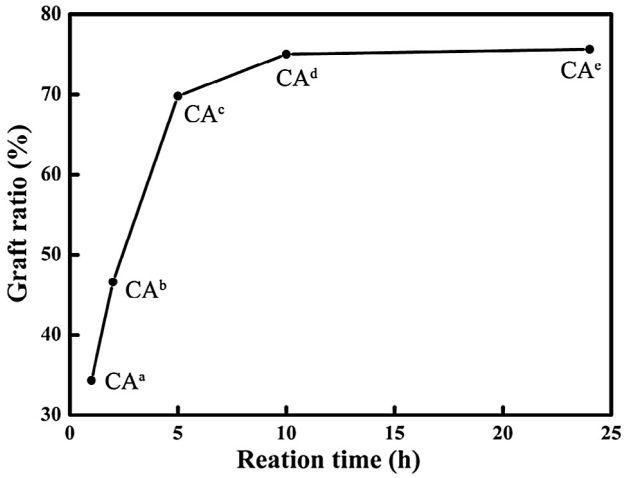

Fig. 3. The effect of reaction time on the grafting ratio.

Table 1
TGA data of CDA, PET and grafting copolymer of CA.

Sample	Initial decomposition temperature/°C	Maximum decomposition temperature/°C	Final decomposition temperature/°C
CDA	268	366	399
CA^a	292	362	403
CA^b	296	362	401
CA^c	297	365	398
CA^d	300	365	396
CA^e	310	363	399
PET	380	445	475

revealed that the diameter of CDA-*g*-PET decreased with the increase of grafting ratio by the same electrospinning process, which might be contributed to the low surface tension of precursor solution with the increase of ratio that generally caused the decrease of diameter.

Mechanical strength is a fundamental requirement for tissues scaffold, From Table 2, it can be observed that the tensile strength of CDA-*g*-PET nanofibers membrane are significant improved compared with CDA nanofibers membrane, indicating that grafted PET onto CDA copolymer will significant improve CDA nanofibers membrane mechanical property. These results are probably attributed to grafting ratio and fiber diameter of nanofibers. In low grafting ratio, mechanical properties of membranes are decided by the CDA with high degree of intramolecular and intermolecular hydrogen bonding interaction and the PET with excellent mechanical properties. In higher grafting ratio, thinner fibers lead to lower tensile strength and higher elongation at break [32].

The wettability of nanofiber membrane was determined by water contact angle. As shown in Table 3, the water contact angles of CDA and PET are 131.25 ± 0.78° and 136.00 ± 1.21°, respectively, (Especially, the sample of PET was fabricated by coating). After grafting PET onto CDA backbone, the WCA of CDA-*g*-PET nanofiber membrane are close to CDA, but slowly increases with grafting ratio. This may be due to the introduction of PET with excellent hydrophobicity to CDA backbone leading to increased surface roughness of CDA-*g*-PET membranes [33].

According to the previous research, a desirable wound dressing should maintain an adequate moisture microenvironment, it will help to accelerate tissue regeneration. Therefore, the assessment of WVTR of membrane is necessary [34]. Table 4 showed that the mean value of WVTR of CA^a, CA^b, CA^c, CA^d, CA^e, CDA and control group were 1538, 1553, 1525, 1580, 1564, 1570 and 1980 $g{\cdot}m^{-2}{\cdot}day^{-1}$, respectively. Furthermore, CA^a, CA^b, CA^c, CA^d, CA^e and CDA nanofiber membranes can reduce the evaporation of water loss by 22.3%, 21.5%, 23.0%, 20.2%, 21.0% and 20.7% to maintain a moisture microenvironment. Especially, the WVTR of CDA-*g*-PET nanofiber membranes are close to CDA, indicating that grafted PET onto CDA backbone didn't change WVTR quality of CDA. These results indicated that CDA-*g*-PET nanofiber membrane can remain a moisture microenvironment when used as wound dressing.

The hemolysis ratio defined as the degree of erythrolysis that blood contact material with disruption of the erythrocyte membrane and release hemoglobin into plasma [35,36]. The lower the hemolysis rate, the better hemocompatibility. Fig. 5 showed that the hemolysis ratios of CDA and CDA-*g*-PET nanofiber membrane are further less than international standard 5% [37], indicating that these nanofiber membrane possessed good blood compatibility. Especially, the hemolysis ratio of CDA nanofiber membrane is 0.39%, which is higher than CDA-*g*-PET nanofiber membrane, indicating that CDA-*g*-PET nanofiber membranes have better hemocompatibility than CDA. In addition, hemolysis ratio decreased with grafting ratio increased, displaying a better hemocompability. The reason for this hemolysis ratio might be grafting of hydrophobic PET onto CDA backbone, the stronger hydrophobic, the lower blood adhesion in surface. Moreover, long side molecular chain will increase roughness of membrane surface and improve hemocompatibility [38].

To assess material biocompatibility, cell culture test on material surface is an effective method [39]. Firstly, the cells were treated with colorant MTT that can transform glycolysis equivalently, and then the cell viability on CDA and CDA-*g*-PET nanofiber membranes with different grafting ratio can be assessed by measuring the optical density (OD) at 490 nm [22,37]. Fig. 6 showed the viability of fibroblast on CDA and CDA-*g*-PET nanofiber membranes after 1, 3 and 7 days of cultured period. At the same time, seeding cells in a complete media without nanofiber membrane were used as the control groups. All nanofiber membrane showed significant increase with incubation time. The cell viability on CDA-*g*-PET nanofiber membrane and CDA nanofiber membrane were not significantly different at 1 d and 3 d. However, cell viability on CDA-*g*-PET nanofiber membrane increased compared with on CDA nanofiber membrane at 7 d. Cell viability on CDA-g-PET nanofiber membrane and CDA nanofiber membrane were beyond 90% at 1 day, demonstrating that grafted PET onto CDA copolymer had low toxicity. It is agreed with that CDA is a kind of good biocompatibility materials in previous report [40]. At 7 d, cell

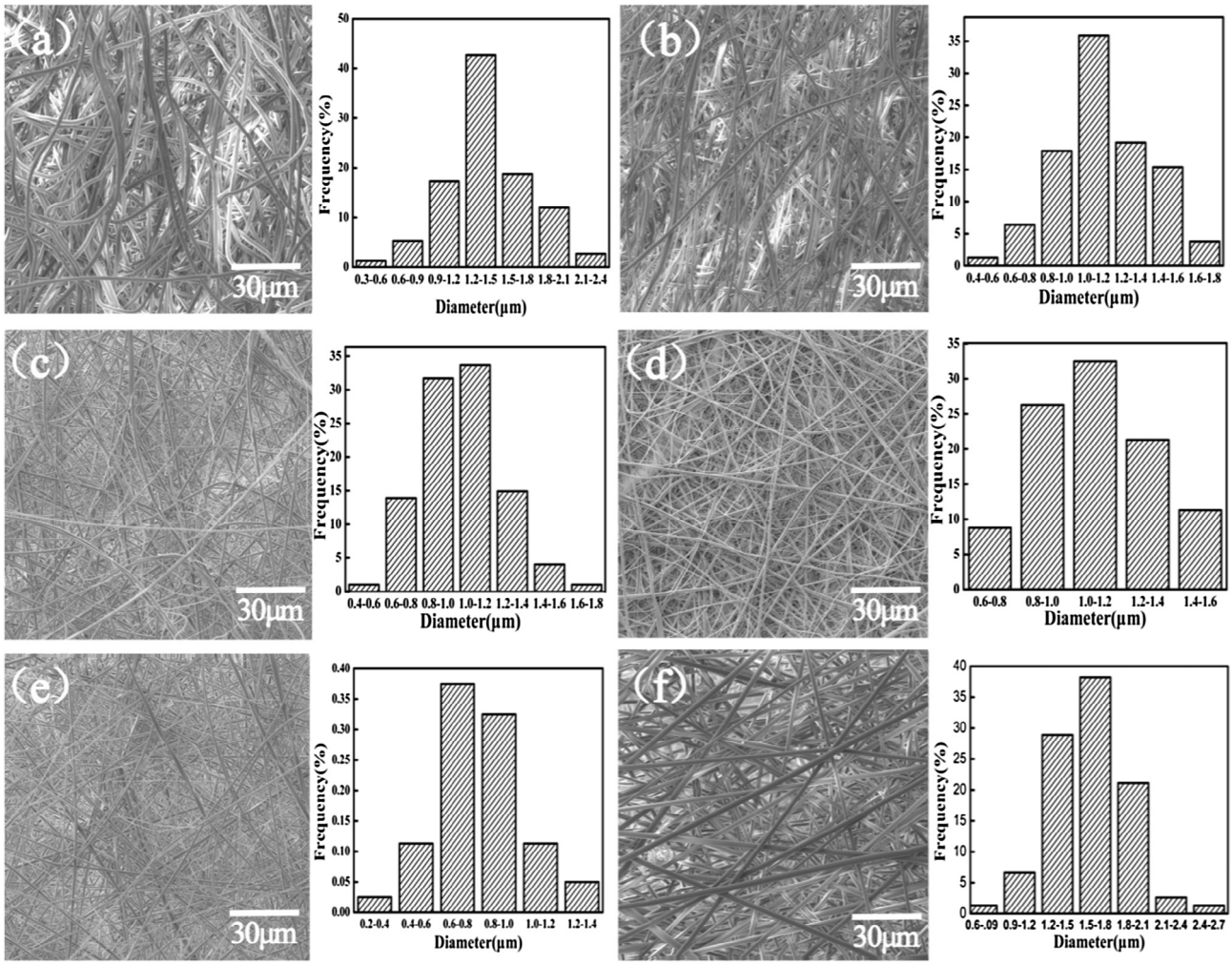

Fig. 4. The SEM images and the pictures of diameter distribution of CDA-*g*-PET and CDA. (a∼f) Represent CA^a, CA^b, CA^c, CA^d, CA^e and CDA respectively.

Table 2
The mechanical properties of CDA and graft copolymers (CA).

Product	CDA	CA^a	CA^b	CA^c	CA^d	CA^e
Tensile strength/MPa	3.17 ± 0.23	10.79 ± 0.45	13.79 ± 0.44	11.53 ± 0.61	10.34 ± 0.26	10.12 ± 0.22
Failure strain/%	2.92 ± 0.12	3.81 ± 0.09	3.65 ± 0.21	3.66 ± 0.21	3.86 ± 0.17	4.16 ± 0.11

Table 3
Water contact angle of CDA, PET and CDA-*g*-PET.

Product	CDA	PET	CA^a	CA^b	CA^c	CA^d	CA^e
Contact angle/°	131.25 ± 0.78	136.00 ± 1.21	133.46 ± 1.03	134.96 ± 0.89	135.75 ± 0.91	135.58 ± 0.72	136.01 ± 0.84

Table 4
Water vapor transmission loss of CDA-*g*-PET, CDA and blank control group.

Product	CA^a	CA^b	CA^c	CA^d	CA^e	CDA	Control group
WVTR/g m^{-2}·day^{-1}	1538 ± 66	1553 ± 49	1525 ± 53	1580 ± 87	1564 ± 65	1570 ± 78	1980 ± 99

viability further increased on CDA-*g*-PET nanofiber membrane compared with CDA nanofiber membrane, because long molecular chain will increase the surface roughness of membranes. Meanwhile, ES membranes can provide a three-dimensional (3D) structure with high surface area and high porous ratio, improving cell attachment and proliferation in interfibrous gap [41,42]. The MTT results demonstrated that CDA-*g*-PET were better than CDA biocompatibility property.

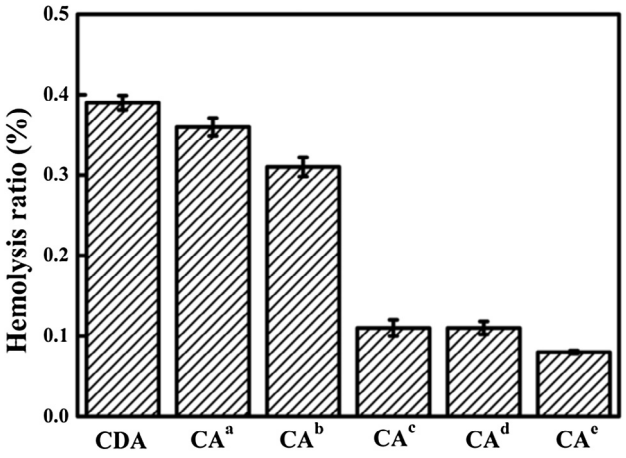

Fig. 5. Hemolysis ratio of CDA and CDA-*g*-PET, respectively.

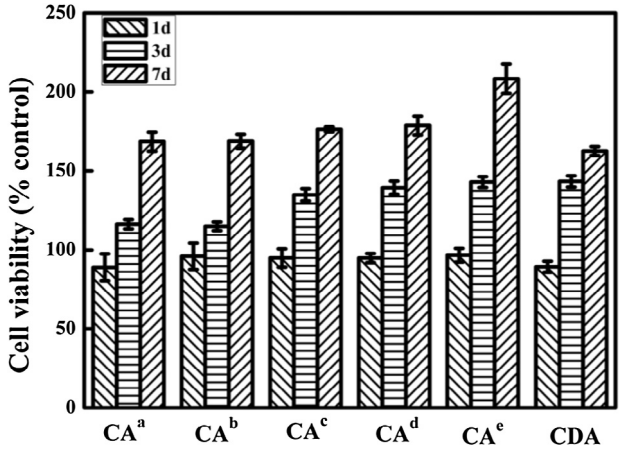

Fig. 6. Fibroblast viability of CDA-*g*-PET and CDA at 1, 3 and 7 day, respectively.

4. Conclusion

In this study, CDA-*g*-PET copolymers were prepared by grafting reaction in homogenous solvent. CDA-*g*-PET has improved heat-resistant ability compared with CDA. Fabricated nanofiber based on CDA-*g*-PET copolymers via electrospinning showed uniform and smooth morphology and fibrous diameter can be adjusted by grafting ratio. Moreover, mechanical strength has been significantly improved compared with CDA nanofiber. The hemocompatibility and biocompatibility of CDA-*g*-PET are better than CDA, meanwhile, nanofiber membrane can keep moisture when used as wound dressing. In summary, novel CDA-based copolymer and CDA-*g*-PET nanofiber membrane are suitable for tissues scaffold.

Acknowledgement

This research was supported by the National Key Research and Development Program (2016YFC1100703).

References

[1] Q. Yu, X. Xu, L. Zhang, J. Cao, C. Deng, Q. Wang, et al., Study on die swell of cellulose diacetate spinning dope at the exit of regular triangular orifice, Fibers Polym. 16 (2015) 105–112.
[2] R. Konwarh, N. Karak, M. Misra, Electrospun cellulose acetate nanofibers: the present status and gamut of biotechnological applications, Biotechnol. Adv. 31 (2013) 421–437.
[3] Rasoul Esmaeely Neisiany, Jeremy Kong Yoong Lee, Saied Nouri Khorasani, Seeram Ramakrishna, Self-healing and interfacially toughened carbon fibre-epoxy composites based on electrospun core-shell nanofibres, J. Appl. Polym. Sci. 134 (2017) 31.
[4] T. Rojanarata, S. Plianwong, K. Su-uta, P. Opanasopit, T. Ngawhirunpat, Electrospun cellulose acetate nanofibers as thin layer chromatographic media for eco-friendly screening of steroids adulterated in traditional medicine and nutraceutical products, Talanta 115 (2013) 208–213.
[5] M. Ye, N.Q. Zhu, Z.B. Ni, W.F. Dong, M.Q. Chen, Preparation and characterization of innovative cellulose diacetate/epoxy resin blends modified by isophorone diamine, J. Appl. Polym. Sci. 133 (2016) 44.
[6] C. Zhu, R.M. Richardson, K.D. Potter, A.F. Koutsomitopoulou, J.S. van Duijneveldt, S.R. Vincent, et al., High modulus regenerated cellulose fibers spun from a low molecular weight microcrystalline cellulose solution, ACS Sustain. Chem. Eng. 4 (2016) 4545–4553.
[7] N. Liu, B. Wang, S. Chen, F. Ke, Y. Chen, Q. Pei, et al., Improving the mechanical properties of cellulose diacetate fibers via using an ionic liquid as processing solvent, RSC Adv. 6 (2016) 1–7.
[8] M. Soyama, M. Iji, Improving mechanical properties of cardanol-bonded cellulose diacetate composites by adding polyester resins and glass fiber, Polym. J. 49 (2017) 503–509.
[9] H. Zou, P.F. Lv, X. Wang, D. Wu, D.G. Yu, Electrospun poly(2-aminothiazole) cellulose acetate fiber membrane for removing Hg(II) from water, J. Appl. Polym. Sci. 134 (2017) 21.
[10] G. Moreira, E. Fedeli, F. Ziarelli, D. Capitani, L. Mannina, L. Charles, et al., Synthesis of polystyrene-grafted cellulose acetate copolymers via nitroxide-mediated polymerization, Polym. Chem. 6 (2015) 5244–5253.
[11] W. Chen, L. Shi, Z. Wang, J. Zhu, H. Yang, X. Mao, et al., Porous cellulose diacetate-SiO_2 composite coating on polyethylene separator for high-performance lithium-ion battery, Carbohydr. Polym. 147 (2016) 517–524.
[12] C. Zhu, T. Nagaishi, J. Shi, H. Lee, P.Y. Wong, J. Sui, et al., Enhanced wettability and thermal stability of a novel polyethylene terephthalate-based poly (vinylidene fluoride) nanofiber hybrid membrane for the separator of lithium-ion batteries, ACS Appl. Mater. Interfaces 9 (2017) 26400–26406.
[13] P. Zhang, F. Han, Y. Li, J. Chen, T. Chen, Y. Zhi, et al., Local delivery of controlled-release simvastatin to improve the biocompatibility of polyethylene terephthalate artificial ligaments for reconstruction of the anterior cruciate ligament, Int. J. Nanomed. 11 (2016) 465–478.
[14] N. Recek, M. Resnik, R. Zaplotnik, M. Mozetic, H. Motaln, T. Lah-Turnsek, et al., Cell proliferation on polyethylene terephthalate treated in plasma created in SO_2/O_2 mixtures, Polymers 9 (2017) 3.
[15] D. Pezzoli, E. Cauli, P. Chevallier, S. Fare, D. Mantovani, Biomimetic coating of cross-linked gelatin to improve mechanical and biological properties of electrospun PET: a promising approach for small caliber vascular graft applications, J. Biomed. Mater. Res. Part A. 105 (2017) 2405–2415.
[16] T. Lan, Gu. Shao Z-q, Zhou Z-w M-j, Wang Y-l, Wang W-j, et al., Electrospun nanofibrous cellulose diacetate nitrate membrane for protein separation, J. Membr. Sci. 489 (2015) 204–211.
[17] K.A. Rieger, H.J. Cho, H.F. Yeung, W. Fan, J.D. Schiffman, Antimicrobial activity of silver ions released from zeolites immobilized on cellulose nanofiber mats, ACS Appl. Mater. Interfaces 8 (2016) 3032–3040.
[18] J. Xue, J. Xie, W. Liu, Y. Xia, Electrospun nanofibers: new concepts, materials, and applications, Acc. Chem. Res. 50 (2017) 1976–1987.
[19] D. Liu, X. Zhang, T. You, Urea-treated carbon nanofibers as efficient catalytic materials for oxygen reduction reaction, J. Power Sources 273 (2015) 810–815.
[20] C.H. Yao, C.Y. Lee, C.H. Huang, Y.S. Chen, K.Y. Chen, Novel bilayer wound dressing based on electrospun gelatin/keratin nanofibrous mats for skin wound repair, Mater. Sci. Eng., C 79 (2017) 533–540.
[21] S. Bhowmick, S. Rother, H. Zimmermann, P.S. Lee, S. Moeller, M. Schnabelrauch, et al., Biomimetic electrospun scaffolds from main extracellular matrix components for skin tissue engineering application – The role of chondroitin sulfate and sulfated hyaluronan, Mater. Sci. Eng., C 79 (2017) 15–22.
[22] K. Yu, X. Zhou, T. Zhu, T. Wu, J. Wang, J. Fang, et al., Fabrication of poly(ester-urethane)urea elastomer/gelatin electrospun nanofibrous membranes for potential applications in skin tissue engineering, RSC Adv. 6 (2016) 73636–73644.
[23] C.J. Thompson, G.G. Chase, A.L. Yarin, D.H. Reneker, Effects of parameters on nanofiber diameter determined from electrospinning model, Polymer 48 (2007) 6913–6922.
[24] B. Zhang, F. Kang, J.-M. Tarascon, J.-K. Kim, Recent advances in electrospun carbon nanofibers and their application in electrochemical energy storage, Prog. Mater Sci. 76 (2016) 319–380.
[25] A. Nicosia, T. Keppler, F.A. Müller, B. Vazquez, F. Ravegnani, P. Monticelli, et al., Cellulose acetate nanofiber electrospun on nylon substrate as novel composite matrix for efficient, heat-resistant, air filters, Chem. Eng. Sci. 153 (2016) 284–294.
[26] S. Tungprapa, T. Puangparn, M. Weerasombut, I. Jangchud, P. Fakum, S. Semongkhol, et al., Electrospun cellulose acetate fibers: effect of solvent system on morphology and fiber diameter, Cellulose 14 (2007) 563–575.
[27] Y. Liu, J. Zhou, L. Chen, P. Zhang, W. Fu, H. Zhao, et al., Highly flexible freestanding porous carbon nanofibers for electrodes materials of high-performance all-carbon supercapacitors, ACS Appl. Mater. Interfaces 7 (2015) 23515–23520.

[28] Y. Li, Y. Xiao, C. Liu, The horizon of materiobiology: a perspective on material-guided cell behaviors and tissue engineering, Chem. Rev. 117 (2017) 4376–4421.
[29] Q. Jiang, W. Zhou, J. Wang, R. Tang, D. Zhang, X. Wang, Hypromellose succinate-crosslinked chitosan hydrogel films for potential wound dressing, Int. J. Biolog. Macromol. 91 (2016) 85–91.
[30] Lipeng Wang, Yu Wang, Fuchen Zhang, Yongping Bai, Liping Ding, Syntheses and properties of the PET-co-PEA copolyester, J. Appl. Polym. Sci. 134 (2017) 36.
[31] H. Chen, W. Ma, Y. Xia, Y. Gu, Z. Cao, C. Liu, et al., Improving amphiphilic polypropylenes by grafting poly(vinylpyrrolidone) and poly(ethylene glycol) methacrylate segments on a polypropylene microporous membrane, Appl. Surf. Sci. 419 (2017) 259–268.
[32] Meenu Teotia, Nazia Tarannum, Rakesh Kumar Soni, Depolymerization of PET waste to potentially applicable aromatic amides: their characterization and DFT study, J. Appl. Polym. Sci. 134 (2017) 31.
[33] J. Deng, S. Yuan, X. Li, K. Wang, L. Xie, N. Li, et al., Heparin/DNA aptamer co-assembled multifunctional catecholamine coating for EPC capture and improved hemocompatibility of vascular devices, Mater. Sci. Eng., C 79 (2017) 305–314.
[34] D. Atila, D. Keskin, A. Tezcaner, Cellulose acetate based 3-dimensional electrospun scaffolds for skin tissue engineering applications, Carbohydr. Polym. 133 (2015) 251–261.
[35] N. Cai, Q. Li, J. Zhang, T. Xu, W. Zhao, J. Yang, et al., Antifouling zwitterionic hydrogel coating improves hemocompatibility of activated carbon hemoadsorbent, J. Colloid Interface Sci. 503 (2017) 168–177.
[36] Z. Fan, B. Liu, J. Wang, S. Zhang, Q. Lin, P. Gong, et al., A novel wound dressing based on Ag/graphene polymer hydrogel: effectively kill bacteria and accelerate wound healing, Adv. Funct. Mater. 24 (2014) 3933–3943.
[37] X. Chen, J. Wang, Q. An, D. Li, P. Liu, W. Zhu, et al., Electrospun poly(L-lactic acid-co-varepsilon-caprolactone) fibers loaded with heparin and vascular endothelial growth factor to improve blood compatibility and endothelial progenitor cell proliferation, Colloids Surf. B: Biointerfaces 128 (2015) 106–114.
[38] Q. Li, F. Tang, C. Wang, X. Wang, Novel mussel-inspired Ti-6Al-4V surfaces with biocompatibility, blood ultra-drag reduction and superior durability, Mater. Sci. Eng., C 76 (2017) 1041–1047.
[39] K. Deshmukh, M.B. Ahamed, R.R. Deshmukh, S.K.K. Pasha, K.K. Sadasivuni, A.R. Polu, et al., Newly developed biodegradable polymer nanocomposites of cellulose acetate and Al_2O_3 nanoparticles with enhanced dielectric performance for embedded passive applications, J. Mater. Sci.: Mater. Electron. 28 (2016) 973–986.
[40] A.C. Mendes, K. Stephansen, I.S. Chronakis, Electrospinning of food proteins and polysaccharides, Food Hydrocolloids 68 (2017) 53–68.
[41] T. Zhu, K. Yu, M.A. Bhutto, X. Guo, W. Shen, J. Wang, et al., Synthesis of RGD-peptide modified poly(ester-urethane) urea electrospun nanofibers as a potential application for vascular tissue engineering, Chem. Eng. J. 315 (2017) 177–190.
[42] M. Zhang, J. Zeng, L. Hu, G. Liu, Y. Ma, Y. Tang, et al., Three-dimensional coating of porous zein/PLLA coaxial nanofiber membranes on surfaces of calcium phosphate cement, Ceram. Int. 43 (2017) 11039–11047.